

min of irradiation showed only 4 (83%).

Reactions of 1 with Dimsyl Anion. Dimethyl sulfoxide (5.86 g, 75 mmol), freshly vacuum distilled from calcium hydride, was added to 75 mmol of potassium amide in 300 mL of NH_3 and stirred for 10 min. Irradiation was begun, and 1 (3.16 g, 20 mmol) was added and rinsed in with 50 mL of ether. After 15 min the mixture was quenched and worked up as usual. GC analysis showed mostly 2-aminopyridine (8) along with a trace of an unidentified pyridine-containing product.

A reaction similar to the above was conducted for 15 min in the dark and produced only 8.

Attempted Reactions of 1 with Other Anions. 2-Bromopyridine (1) or 2-chloroquinoline (4) (20 mmol) was added to solutions of 75 mmol of potassium acetylde, potassium phenylacetylde, and potassium phthalimide, each prepared from 75

mmol of potassium amide in 300 mL of NH_3 . The reactions were irradiated for 120 min, quenched on ammonium chloride, and worked up as usual. GC analysis showed only unreacted 1 or 4.

Registry No. 1, 109-04-6; 2, 75782-32-0; 3, 5005-36-7; 4, 612-62-4; 5, 22297-12-7; 6, 59175-44-9; 6 carbanion, 21438-99-3; 7, 2739-97-1; 8, 504-29-0; 9, 14068-28-1; 12, 72248-92-1; 13, 22200-36-8; 14, 85736-21-6; 15, 78903-70-5; 16, 19524-06-2; 17, 60776-05-8; 19, 85736-22-7; 20, 54043-02-6; 21, 3111-54-4; NH_3 , 7664-41-7; KNH_2 , 17242-52-3; K, 7440-09-7; $\text{Fe}(\text{NO}_3)_3$, 10421-48-4; CH_3CN , 75-05-8; potassium phenylacetylene, 1122-79-8; potassium phthalimide, 107-82-4; potassium acetylene, 1111-63-3; di-*tert*-butyl nitroxide, 2406-25-9; phenylacetonitrile, 140-29-4; cyanoacetone, 2469-99-0; *o*-aminobenzaldehyde, 529-23-7; 4-picoline, 108-89-4; dimsyl anion, 13810-16-7; dimethyl sulfoxide, 67-68-5.

MINDO/3-Derived Geometries and Energies of Alkylpyridines and the Related *N*-Methylpyridinium Cations¹

Jeffrey I. Seeman*

Philip Morris U.S.A. Research Center, Richmond, Virginia 23225

John C. Schug* and Jimmy W. Viers*

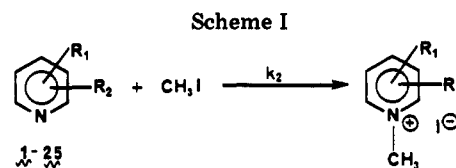
Department of Chemistry, Virginia Polytechnic Institute & State University, Blacksburg, Virginia 24061

Received August 4, 1982

The structures of 25 alkyl-substituted pyridines and their corresponding *N*-methylpyridinium cations were calculated by using GEOMO/RV, utilizing semiempirical all-valence electron (MINDO/3) self-consistent-field procedures. The effects of substituents on the ring systems were examined with particular attention focused on the changes in the aromatic ring bond angles. The energy of methylation for these 25 pyridines was calculated by subtracting the total energy of each pyridine-free base from the total energy of the corresponding *N*-methylpyridinium cation. An excellent correlation was obtained between this calculated energy of methylation and Brown's experimental heats of trifluoroborations for the same pyridines; implications of this correlation are discussed. Nonadditive structural parameters and energetic effects are calculated and evaluated.

During the past year we^{2,3} have been investigating the Menshutkin reaction of alkylpyridines (Scheme I) with the help of the semiempirical MINDO/3 all-valence-electron theory.⁴ For a series of 2-alkylpyridines, we have found that the nonadditive part of the second-order methylation rate constant was highly correlated with the molecular position of the 2-substituent.² This finding is of importance to the evaluation of structure-reactivity relationships in the Menshutkin reaction. In a subsequent study, we constructed model transition states for a series of 21 pyridines and used the MINDO/3 theory to estimate relative activation energies.³ An excellent Arrhenius-type correlation was found between the logarithms of the relative methylation rate constants and the calculated relative activation energies for systems which span over four orders of magnitude in alkylation rate.

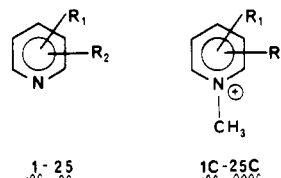
These two studies incorporated complete geometry optimization for the free bases and for the model transition states. A sizeable set of data was, therefore, generated relative to the effect of alkyl substituents on pyridine ring and substituent geometry. We decided to extend the study to also determine the geometries and relative energies of



the series of product *N*-methylpyridinium ions. In so doing, we have searched for relationships between structure, molecular energy, and geometry. In the present paper, we present these results which are important since there is little systematic information regarding the effects of alkyl substituents on aromatic ring structure, bond angles, and bond lengths.⁵

Results and Discussion

The 25 pairs of compounds chosen for study (1-25 and 1C-25C; see Table I) incorporate both a wide range of



(1) For the previous paper in this series, see: Chavdarian, C. G.; Seeman, J. I. *Tetrahedron Lett.* 1982, 23, 2519-2522.

(2) Seeman, J. I.; Galzerano, R.; Curtis, K.; Schug, J. C.; Viers, J. W. *J. Am. Chem. Soc.* 1981, 103, 5982-5984.

(3) (a) Viers, J. W.; Schug, J. C.; Seeman, J. I. *J. Am. Chem. Soc.* 1982, 104, 850-851. (b) Schug, J. C.; Viers, J. W.; Seeman, J. I., submitted for publication.

(4) (a) Bingham, R. C.; Dewar, M. J. S.; Lo, D. H. *J. Am. Chem. Soc.* 1975, 97, 1294-1301. (b) Bingham, R. C.; Dewar, M. J. S.; Lo, D. H. *J. Am. Chem. Soc.* 1975, 97, 1302-1306.

(5) See, for example: (a) Domenicano, A.; Schultz, G.; Kolonits, M.; Hargittai, I. *J. Mol. Struct.* 1979, 53, 197-209. (b) Domenicano, A.; Vaciago, A. *Acta Crystallogr., Sect. B* 1979, B35, 1382-1388 and additional papers in this series. (c) Pang, F.; Boggs, J. E.; Pulay, P.; Fogarasi, G. *J. Mol. Struct.* 1980, 66, 281-287. (d) Allen, F. H. *Acta Crystallogr., Sect. B* 1981, B37, 900-906.

Table I. Chemical Reactivity Data and GEOMO (MINDO/3)-Derived Activation Energies, Energies of Reaction, Ring Geometry Parameters, and the Corresponding Nonadditivity (NA) Values for 1-25 and 1C-25C^x

compd	no.	k_{rel}^a	S^b	methylation reaction			geometry parameters			BF ₃ reaction	
				$\Delta E^{\ddagger c}$	$\Delta E^{\ddagger}(NA)^b$	ΔE_M^d	ΔE_M^d	$\Delta E_M(NA)^b$	$\delta < FBb,e$	$\delta < Cb,e$	$\Delta H_{BF_3}^{\circ f}$
pyridine	1	1		0		0				0	1.7
2-methylpyridine	2	0.47		1.74		3.3					
3-methylpyridine	3	2.1		-0.881		-0.87				-0.3	-0.3
4-methylpyridine	4	2.2		-2.10		-2.7				-0.5	-0.5
2-ethylpyridine	5	0.22		1.62		3.2				2.3	2.3
3-ethylpyridine	6	2.22		0.563		-0.60				-0.2	-0.2
2-isopropylpyridine	7	0.071		1.54		3.5				3.3	3.3
3-isopropylpyridine	8	2.4		-1.34		-1.4				-0.3	-0.3
3-tert-butylpyridine	9	0.00023		8.21		10.6				10.2	10.2
2,3-dimethylpyridine	10	2.8		-1.97		-2.1				-0.6	-0.6
2,4-dimethylpyridine	11	0.57	0.58	2.16	1.30	4.3	1.9	2.4	1.9	1.3	1.3
2,5-dimethylpyridine	12	1.1	1.1	-0.387	-0.023	0.70	0.1	0.11	0.35	0.8	0.8
2,6-dimethylpyridine	13	1.1	1.1	0.953	0.094	2.6	0.2	0.06	0.32	0.8	0.8
2,4,6-trimethylpyridine	14	0.042	0.19	5.47	1.99	8.3	1.7	0.26	1.1	7.5	4.1
2-methyl-3-ethylpyridine	15	0.11	0.22	4.57	3.19	7.3	3.4	1.14	1.6	6.5	3.6
2-methyl-5-ethylpyridine	16	0.48	0.48	2.62	1.44	5.0	2.3	3.2	3.4	1.6	0.1
2-methyl-3-isopropylpyridine	17	1.1	1.1	0.385	-0.795	2.0	-0.7	1.0	0.85	0.7	-0.8
2-methyl-5-isopropylpyridine	18	0.51	0.46	3.07	2.67	4.6	2.7	3.5	3.1	2.0	0.6
2-methyl-3-tert-butylpyridine	19	1.2	1.1	0.387	0.013	2.1	0.2	0.22	0.57	0.9	-0.5
2-methyl-5-tert-butylpyridine	20	0.33	0.25	3.34	3.57	5.3	4.1	6.3	6.3	3.1	2.0
2-ethyl-3-methylpyridine	21	1.3	1.0	-0.025	0.257	1.5	0.3	0.10	0.31	0.8	-0.3
2-ethyl-5-methylpyridine	22	0.24	0.52	2.87	2.13	5.3	3.0	3.1	3.0	2.4	0.4
2-isopropyl-3-methylpyridine	23	0.54	1.2	1.22	0.477	3.0	0.7	0.18	0.42	1.5	-0.5
2-isopropyl-5-methylpyridine	24	0.0031	0.021	5.29	4.64	8.3	5.7	5.3	4.5	6.5	3.7
2-isopropyl-3,5-methylpyridine	25	0.17	1.1	0.698	0.044	2.7	0.1	0.49	0.34	2.5	-0.3

^a In nitrobenzene at 25 °C. Kinetic data were taken entirely from the work of Brown et al.⁶ in order to avoid slight differences in relative rates of reaction for methylations run in other solvents. ^b Additivity factors were calculated by using LFER. Perfect additivity for these parameters is a value of zero, except for S, the nonadditive kinetic factor, where perfect additivity is a value of one. See text for discussion. ^c MINDO/3-derived activation energy obtained by using the transition-state model described in ref 3. ^d MINDO/3-derived energy of methylation. Derived from eq 4 and 5. ^e The parameter $\delta <$ is derived as follows: for 2C-10C, the "standard" effect of each monosubstituent was determined relative to 1C; for each polysubstituted cation, a theoretical additive geometry was derived by summing the effects at each angle caused by the substituents by using the "standard" values. The sum of the absolute differences for all the internal angles between the "observed MINDO/3" geometry and the "additive" geometry was then calculated and is $\delta <$. A similar procedure was performed for 2-25 relative to 1. ^f From ref 6c-e. ^g Units: ΔE values in kilocalories per mole, δ values in degrees, and ΔH values in kilocalories per mole.

Table II. Comparison of Experimental Data with GEOMO (MINDO/3)-Derived Molecular Geometries

atoms	pyridine [x = :], obsd ^a (calcd)	N-methylpyridinium [X = C ⁺ _M H ₃ I ⁻], obsd ^b (calcd ^c)
Bond Lengths, Å		
NC ₂	1.34 (1.34)	1.40 (1.36)
C ₂ C ₃	1.39 (1.41)	1.36 (1.40)
C ₃ C ₄	1.39 (1.41)	1.40 (1.41)
NC _M		1.46 (1.45)
Bond Angles, deg		
C ₂ NC ₆	116.9 (119.9)	121 (120.4)
NC ₂ C ₃	123.8 (122.5)	120 (120.8)
C ₃ C ₃ C ₄	118.5 (117.8)	120 (119.7)
C ₃ C ₄ C ₅	118.4 (119.6)	118 (118.5)

^a For pyridine (by microwave), see: Mata, F.; Quintana, M. J.; Sorensen, G. O. *J. Mol. Struct.* 1977, 42, 1-5.

^b For N-methylpyridinium iodide (by x-ray), see: LaLancette, R. A.; Furey, W.; Costanzo, J. N.; Hemmes, P. R.; Jordan, F. *Acta Crystallogr., Sect. B* 1978, B34, 2950-2953. In the crystal, the N-methylpyridinium cation is asymmetric due to the influence of two I⁻ in the crystal lattice. The results cited above are the average values from the X-ray determined structure. ^c For N-methylpyridinium cation.

reactivity (greater than four orders of magnitude) with regard to methylation and varied substituent patterns (2-alkyl-, 3-alkyl-, 2,3-dialkyl-, 2,5-dialkyl-, and 2,6-dialkylpyridines). Eight of these pyridines methylate in a nonadditive kinetic fashion;^{2,6} i.e., the effect of multiple substituents on the reactivity of a substrate is not equal to the effect predicted on the basis of the independent influence of each substituent.

The structures of the free bases and the N-methylpyridinium cations were optimized and the energies determined by using the GEOMO/RV program^{7a} which incorporates the MINDO/3 algorithm for the SCF calculations and the procedure developed by Rinaldi^{7b} for structure optimization. We optimized all structural parameters without symmetry restrictions. In a number of test cases, the final optimized parameters (except for dihedral angles on alkyl substituents) were shown to be independent of reasonable initial values chosen.

GEOMO (MINDO/3)-generated structures have been validated for a number of simple heteroaromatic compounds for which experimental structural data are available.²⁻⁴ The ring geometry of pyridine itself has previously been shown to be well calculated by the GEOMO (MINDO/3) algorithms (Table II). We find that the completely optimized geometry of N-methylpyridinium cation is reasonably close to the average structure obtained by X-ray

Table III. Comparison of Experimental Heats of Formation with GEOMO (MINDO/3)-Derived Heats of Formation for Pyridines

compd	ΔH_f° (gas), kcal mol ⁻¹	
	exptl ^a	calcd
pyridine	34.55	34.13 ^b
2-methylpyridine	23.70	22.46
3-methylpyridine	25.42	27.17
4-methylpyridine	24.41	27.77
2,3-dimethylpyridine	16.32	18.17
2,4-dimethylpyridine	15.27	16.23
2,5-dimethylpyridine	15.88	15.32
2,6-dimethylpyridine	14.03	10.81
3,4-dimethylpyridine	16.74	23.93
3,5-dimethylpyridine	17.40	20.29

^a From the "selected values" chosen by Cox and Pilcher (Cox, J. D.; Pilcher, G. "Thermochemistry of Organic and Organometallic Compounds"; Academic Press: New York, 1970). ^b Identical value reported by Dewar in ref 4b.

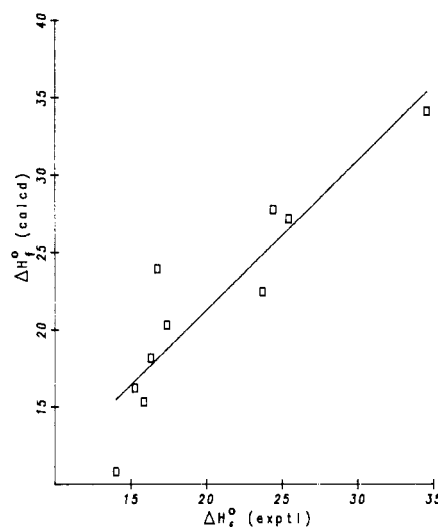


Figure 1. Relationship between GEOMO (MINDO/3)-calculated heats of formation and experimental ΔH_f° (kcal mol⁻¹). See Table III and eq 1.

crystallographic analysis of N-methylpyridinium iodide (Table II).

The structural changes that occur in the pyridine skeleton on methylation are all predicted in the correct direction, but the magnitudes of some of the major changes are apparently underestimated by the calculations. (Note, in particular, NC₂, \angle C₂NC₆, and \angle NC₂C₃.) However, these comparisons may not be completely appropriate because the experimental data for the cation are from a study of the crystalline N-methylpyridinium iodide in which the N-methylpyridinium cation is asymmetric due to the influence of two nearby iodide ions (see Table II).

We have compared the MINDO/3-derived heats of formation with the available experimental data (cf. Table III) and have found a significant correlation, as shown in eq 1. Note that the slope of the relationship described

$$\Delta H_f^\circ(\text{calcd}) = 0.979 \Delta H_f^\circ(\text{exptl}) + 1.89 \quad (1)$$

$$r = 0.909; p = 0.00050; n = 10;$$

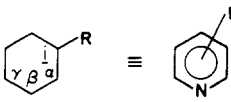
$$\text{std dev of residuals} = 3.06$$

by eq 1 is essentially unity. As can be seen from Figure 1, the deviations between the calculated and experimental ΔH_f° are large, consistent with Dewar's conclusion that MINDO/3-derived ΔH_f° values are satisfactory, though

(6) (a) Brown, H. C.; Cahn, A. *J. Am. Chem. Soc.* 1955, 77, 1715-1723. (b) Brown, H. C.; Gintis, D.; Domash, L. *Ibid.* 1956, 78, 5387-5394. (c) Bank, S. Ph.D. Dissertation, Purdue University, West Lafayette, IN, 1960. See, in particular, the summary of data from Ph.D. Dissertations of J. Donahue (1957), M. S. Howie (1959), D. H. McDaniel (1954), H. Podall (1955), and J. S. Olcott (1957), all from the H. C. Brown group, Purdue University, in the appendix of the Bank Dissertation. (d) Brown, H. C. "Boranes in Organic Chemistry"; Cornell University Press: Ithaca, New York, 1972; Chapters V-VIII. (e) Brown, H. C. *J. Chem. Educ.* 1959, 36, 424-431. (f) Brown, H. C. *J. Chem. Soc.* 1956, 1248-1268.

(7) (a) Schmidling, D. *QCPE* 1978, 11, 350. (b) Rinaldi, D. *Comput. Chem.* 1976, 1, 109-114.

Table VI. Effect of Monosubstitution on Alkylpyridines



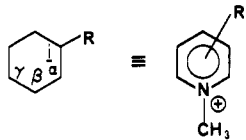
R	change in internal angle, ^a deg			
	<i	<α	<β ^b	<γ
Me	-4.3	2.5	0.08	-0.74
Et	-4.5	2.6	0.17	-0.87
<i>i</i> -Pr	-4.9	2.8	0.14	-1.0
<i>t</i> -Bu	-6.1	3.5	0.27	-1.5

^a Relative to R = H. Average values given for 2-, 3-, and 4-substitution. For 2- and 3-substitution, the angular effects are not symmetrical with respect to the nitrogen atom. ^b Large range of values were obtained.

sometimes encompassing specific exceptions.⁴ Kao and Allinger later showed that molecular mechanics algorithms produced more accurate theoretical ΔH°_f values for *non-heterocyclic* aromatic systems than MINDO/3.⁸ Although some recent efforts⁹ have been devoted to the development of appropriate force fields for nitrogenous compounds, there is much room for progress in the development of force fields for aromatic nitrogenous systems.⁸ Warshel and Lippicirella recently reported an additional semi-empirical procedure, QCFF/PI, for heteroaromatic systems and applied it to nonsubstituted monocyclic nitrogenous compounds.¹⁰ While the MINDO/3-derived geometry of pyridine is somewhat closer to the observed geometry than the QCFF/PI-derived geometry,¹⁰ there are insufficient data available to compare the utility of MINDO/3 with QCFF/PI for substituted systems.

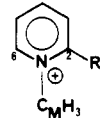
The relatively few experimental data available for comparison in Table III and Figure 1 make it difficult to draw firm conclusions regarding the reliability of heats of formation calculated by the MINDO/3 method for these systems. Trends in the calculated ΔH°_f seem to be generally reliable. However, closer study of the numbers in Table III indicates that there *may* in fact be difficulties in two areas: (a) the interactions between the nitrogen atom and methyl groups at the ortho positions are possibly predicted to be too attractive in nature, and/or (b) the repulsive interactions between methyl groups on adjacent ring carbons may be overemphasized. Unfortunately, there is also a lack of experimental ΔH°_f values for more highly substituted pyridines than those listed in Table III. However, as will be shown later, it appears that differences in ΔH°_f for free base-cation pairs are reasonably calculated by the MINDO/3 method.

The derived geometries for 1-25 and 1C-25C are listed in Tables IV and V (see the paragraph at the end of the paper regarding supplementary material). The effects of monosubstitution on the geometry of the pyridine free bases and the *N*-methylpyridinium cations are summarized in Tables VI and VII. Definite trends can be seen for both the free bases and the cations as the substituent becomes increasingly bulky.¹¹ In our discussions, we will concen-

Table VII. Effect of Monosubstitution on *N*-Methylpyridinium Cations^a


R	change in internal angle, ^a deg			
	<i	<α	<β ^b	<γ
Me	-4.9	2.7	0.20	-0.97
Et	-5.3	3.0	0.30	-1.2
<i>i</i> -Pr	-5.7	3.2	0.33	-1.3
<i>t</i> -Bu	-7.3	3.9	0.53	-1.9

^a Mean values, relative to R = H. Average values given for 2-, 3-, and 4-substitution. For 2- and 3-substitution, the angular effects are not symmetrical with respect to the nitrogen atom. ^b Large range of values were obtained.

Table VIII. Effect of α -Substitution on the Orientation of the N-CH₃ Group


R	change in angle, ^a deg		
	<C ₂ NC _M	<C ₆ NC _M	<C ₂ NC ₆
Me	2.3	-4.1	1.8
Et	2.6	-4.6	2.0
<i>i</i> -Pr	3.1	-5.3	2.2
<i>t</i> -Bu	5.9	-8.2	2.6

^a Relative to R = H.

trate primarily on the effect of substituents on bond angles rather than bond lengths, as it is well-known that the former are more sensitive to substituent-induced change than the latter due to the relative magnitude of the force constants for bond angle deformation contrasted to bond length deformation.¹²

For example, consider the internal ring angles. The maximum effect is observed at the ipso carbon for both the pyridine free bases and the pyridinium cations, where $\angle i$ decreases by an average 4.3° (4.9° for the pyridinium cations) for a methyl substituent to an average decrease of 6.1° (7.3°) for a *tert*-butyl group (see Tables VI and VII). Of course, as the pyridine ring nucleus remains essentially planar, the sum of the internal angles must remain essentially 720°; i.e., as the ipso angle decreases, some of the other angles must increase, most notably (Tables VI and

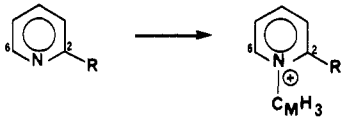
(8) Kao, J.; Allinger, N. L. *J. Am. Chem. Soc.* 1977, 99, 975-986. See also: Osawa, E.; Musso, H. *Top. Stereochem.* 1982, 13, 117-193.

(9) Profeta, S., Jr. Ph.D. Dissertation, University of Georgia, Athens, GA, 1978. We thank Prof. N. L. Allinger for making portions of this dissertation available to us.

(10) Warshel, A.; Lippicirella, A. *J. Am. Chem. Soc.* 1981, 103, 4664-4673.

(11) (a) For these molecules studied herein, especially 5-25 and 2C-25C, the large number of degrees of freedom suggest that extreme care be used before a definite assignment is made for the ground-state equilibrium geometry of a molecule. Ignoring the inherent limitations of any theoretical treatment, we emphasize that numerous local minima abound to confound chemical interpretation, especially for torsional angles involving singly bonded atoms with low barriers to rotation. In some cases, we have started a series of calculations for a particular compound at different geometries, "optimizing" all parameters. In other cases, we have intentionally held one particular parameter constant (usually a dihedral angle of a ring substituent) and "optimized" all other parameters, thereby generating rotational energy barrier information. The excellent correlations obtained suggest that the trends observed are real and useful for chemical interpretations and extrapolations. These warnings are considered general for most types of complete geometry optimization routines, and we feel that geometry optimization offers considerably more insight than work in which *standard* bond lengths, bond angles, and geometries are chosen.^{11b} (b) Boyd, D. B.; Lipkowitz, K. B. *J. Chem. Educ.* 1982, 59, 269-274.

(12) Schug, J. C. "Introductory Quantum Chemistry"; Holt, Rinehart, and Winston, Inc.: New York, 1972; Chapter 11.

Table IX. Pyridine Ring α -Carbon Displacements upon Quaternization


substrate	$\Delta d_{NC_2},^a$ Å	$\Delta d_{NC_6},^a$ Å	$\Delta \angle C_M NC_2,$ deg	$\Delta \angle C_M NC_6,$ deg
pyridine	0.0289	0.0289	-0.25	-0.25
2-picoline	0.0326	0.0485	3.45	-2.95
2- <i>tert</i> -butylpyridine	0.0356	0.0463	7.66	-6.44

^a d is the bond length of the specified bond.

VII) the α angle. We emphasize that the changes in internal angles listed in Tables VI and VII are the average values for 2-, 3-, and 4-substituted substrates; for 2- and 3-substituents, the angular effects are *not* symmetrical with respect to the pyridine nitrogen. For example, for 2-ethylpyridine (relative to pyridine), $\angle C_2 NC_6$ increases 2.9° while the other α angle $\angle C_2 C_3 C_4$ increases 2.1°.

These substituent-induced changes in the internal pyridine ring angles can be attributed to steric and bonding effects, and it is not possible to separate the two at this time. If steric repulsion were the only factor involved, the change in the ipso angle for a *tert*-butyl substituent relative to that for a methyl group might be expected to be somewhat larger than is actually found. Moreover, the decrease by several degrees in the ipso angle is consistent with a tendency to draw additional s character into the bonding hybrid of the ring carbon atom when the exocyclic C-H bond is replaced by a C-C bond.¹² Our calculations indicate that the ipso angle decreases upon substitution. The decrease is accompanied by a change in hybridization at the ring carbon, and the change is larger the bulkier the substituent group. It is not possible to determine from the calculations what is cause and what is effect in terms of steric and rehybridization bonding effects on the ipso angle.

It is interesting to note the similarities of the entries in Tables VI and VII. To a very good approximation, certainly within the accuracy of the calculations, the effects of alkyl substitution on internal ring angles are the same in the free base and the *N*-methylpyridinium ion.

Table VIII illustrates the nonadditivity of structural parameters in terms of the effect of a bulky 2-substituent on the orientation of the *N*-methyl group in the quaternized systems. For the unsubstituted *N*-methylpyridinium cation (1C), the methyl carbon C_M falls on the C_4 -N axis. However, as the substituent on an α -carbon increases in size, the orientation of the *N*-methyl group relative to the pyridine ring nucleus changes rather dramatically (cf. Table VIII). Due to the α effect illustrated in Table VII, the internal $\angle C_2 NC_6$ changes slightly, but the external $\angle C_2 NC_M$ and $\angle C_6 NC_M$ are more significantly affected. Thus, for *N*-methyl-2-*tert*-butylpyridinium cation, $\angle C_M NC_4 = 171.9^\circ$, significantly less than 180° for the parent cation 1C.

It is of interest to consider the particular atomic displacements that are employed by the cations to reduce crowding in the neighborhood of nitrogen. These displacements were generated by assuming that at very large distances the approaching methyl carbon follows a linear path in the plane of the ring which bisects the original external $\angle C_2 NC_6$ angle. If the nitrogen is kept stationary and the methyl group is moved up to its equilibrium position, one can calculate the changes that take place in the NC_α bond lengths and in the $C_M NC_\alpha$ angles. Table IX shows these displacements for the ortho carbons of

pyridine, 2-picoline, and 2-*tert*-butylpyridine.

In pyridine, the distortions are small and symmetric. The primary displacement of the α -carbons is along the NC_α bond, but there is sufficient lateral motion so that the $\angle C_2 NC_6$ angle increases by almost 0.5° upon quaternization.

For the other two cases, the distortions increase in magnitude from pyridine and are unsymmetrical. In both 2-picoline and 2-*tert*-butylpyridine, the displacements consists of NC_α bond extensions superimposed on a rotation of the entire pyridine molecule in such a way as to decrease the repulsive methyl-*N*-2-substituent interactions. As far as changes in the $\angle C_2 NC_6$ angles are concerned, the motions of carbons C_2 and C_6 are in opposite directions. The substituted carbon C_2 tends to move so as to decrease the $\angle C_2 NC_6$ angle, but the displacement of C_6 tends to increase the angle. The net result is that there is generally a fairly small change in this angle upon quaternization.

These arguments must not be extended too far, because steric forces are not the only operatives here. The specific bonding requirements of the C_M -N moiety as well as of the entire pyridine ring also have to be satisfied. The overall picture is thus quite complicated.

As an additional test of the ability of the MINDO/3 method to probe the detailed structural changes in these compounds, we have calculated the internal rotational barrier of the CH_3 group in 2-picoline. This barrier was found via microwave spectroscopy to have a height of 258 cal/mol.¹³ Our calculations were carried out by fixing the dihedral angle of one of the methyl C-H bonds with respect to the plane of the pyridine ring at a series of values and, at each location, optimizing all other variables. This yielded a barrier height of 207 cal/mol, which compares favorably with the experimental value, with an energy minimum at the $HC_{2a}C_2N$ dihedral angle of 0° and a maximum at 60° .

To investigate how much rotational barriers are affected by buttressing effects, we have made similar calculations for 2,3-lutidine and 2-methyl-3-*tert*-butylpyridine. The barrier heights in these compounds were found to be 877¹⁴ and 806 cal/mol,¹⁵ respectively. The difference between these numbers is not significant, though both barriers are about fourfold greater than that for 2-picoline. It should be noted that even in 2-methyl-3-*tert*-butylpyridine, our

(13) Dreizler, H.; Rudolph, H. D.; Mäder, H. Z. *Naturforsch.*, A 1970, 25A, 25-35.

(14) For 2,3-lutidine, the rotational minimum calculated is as follows: $\tau(HC_{2a}C_2N)$ dihedral angles of 2° , 122° , and 241° ; $\tau(HC_{3a}C_3C_2)$ dihedral angles of 76° , 195° , and 316° . The rotational maximum calculated is as follows: $\tau(HC_{2a}C_2N)$ dihedral angles of -30° , 92° , and 212° ; $\tau(HC_{3a}C_3C_2)$ dihedral angles of 48° , 168° , and 288° .

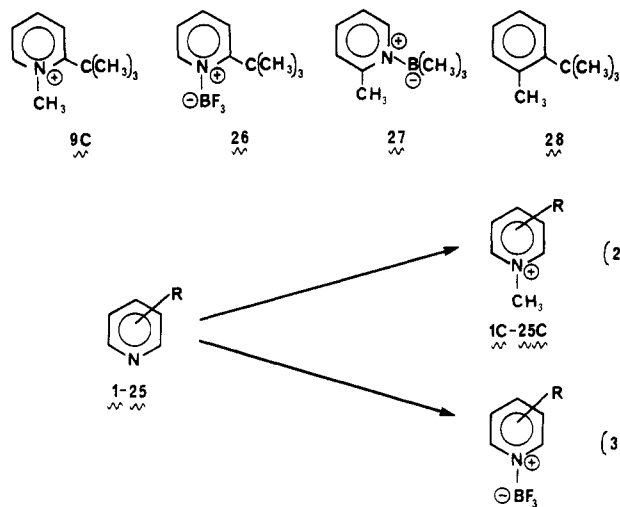
(15) For rotation of the *tert*-butyl group in 2-methyl-3-*tert*-butylpyridine, the rotational minimum calculated is as follows: $\tau(C_{3a}C_{3a}C_3C_2)$ dihedral angles of 64° , 183° , and 302° . The rotational maximum calculated is as follows: $\tau(C_{3a}C_{3a}C_3C_2)$ dihedral angles of 4° , 124° , and 244° . As the *tert*-butyl groups rotates, the dihedral angles $\tau(HC_{2a}C_2N)$ remain essentially stationary at 5.5° , 125° , and 245° .

calculations indicate that the substituents are sufficiently separated that cooperative motions of the two groups are not observed; the methyl group stays essentially stationary as the *tert*-butyl group rotates past it.

Some Observations on Energetics

The Menschutkin reaction of substituted pyridines continues to play a major role in the evaluation of steric and electronic factors in organic processes.¹⁶ Within the last few years, important studies have been reported which focus attention on ground-state structural effects² on reactivity as well as the location and nature of the transition state in the alkylation of substituted pyridines.^{3,17-19} The MINDO/3 calculations performed for 1-25 and 1C-25C discussed above can be utilized to examine a variety of features related to reactivity of pyridines in general and to the Menschutkin reaction in particular. In this section, we will consider two topics dealing with pyridine reactivity: (a) we will compare the MINDO/3-derived energetics for the alkylation of 1-25 with related experimental data; (b) we will evaluate the additivity of these energy parameters.

As a central feature in their classical investigations of steric effects, Brown and his students quantified steric strain in transition states by studying homomorphous molecular addition compounds.⁶ [For example, 9C, 26, and 27 are homomorphs of *o*-*tert*-butyltoluene (28).] They obtained a very comprehensive set of experimental data for the methylation and trifluoroboration of a large series of alkylpyridines (1-25).⁶ Compare the formation of the homomorphous systems in eq 2 and 3.



We calculated a MINDO/3 total energy for each geometry-optimized structure for 1-25 [$E(\text{free base})$] and for 1C-25C [$E(\text{cation})$]. The calculated relative energy of

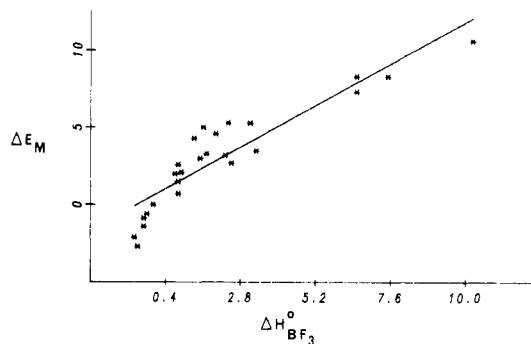


Figure 2. Relationship between GEOMO (MINDO/3)-calculated relative energy of methylation and the relative heat of trifluoroboration (kcal mol^{-1}) for 1-25 (see eq 6).

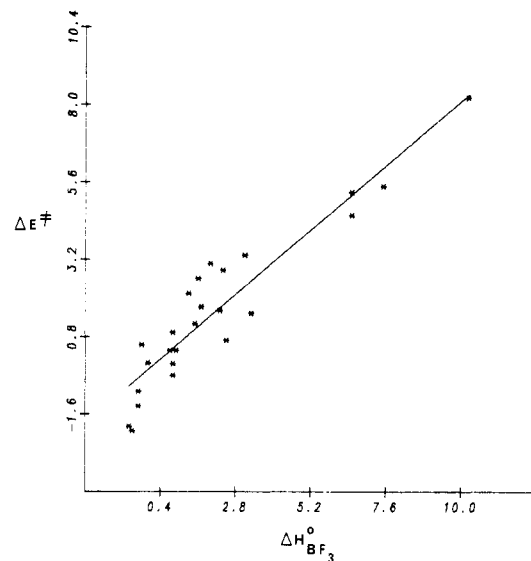


Figure 3. Relationship between GEOMO (MINDO/3)-calculated relative activation energy for methylation and the relative heat of trifluoroboration (kcal mol^{-1}) for 1-25 (see eq 7).

methylation (ΔE_M) for 1-25 relative to pyridine was then derived by using eq 4 and 5 (Table I).

$$\delta E_M = E(\text{cation}) - E(\text{free base}) \quad (4)$$

$$\Delta E_M(i) = \delta E_M(i) - \delta E_M(\text{pyridine}) \quad (5)$$

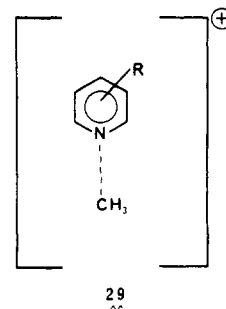
We then correlated ΔE_M with the corresponding relative experimental⁶ heats of reaction ($\Delta H^\circ_{\text{BF}_3}$, eq 3) for the analogous reactions described by eq 2. For the 25 reactions studied, we obtained a good correlation between the experimental heats of reaction of 1-25 with BF_3 and the calculated heats of methylation for these same substances (cf. Figure 2 and eq 6).

$$\Delta H^\circ_{\text{BF}_3} = 0.729\Delta E_M - 0.067 \quad (6)$$

$$r = 0.914; p = 0.00001; n = 25;$$

$$\text{std dev of residuals} = 1.08$$

We have also used the model methylation transition state (TS) described by us earlier³ (cf. 29) to calculate the



(16) (a) Zoltewicz, J. A.; Deady, L. W. *Adv. Heterocycl. Chem.* **1978**, *22*, 72-121. (b) Tomasik, P.; Johnson, C. D. *Ibid.* **1976**, *20*, 1-64. (c) Arnett, E. M.; Reich, R. *J. Am. Chem. Soc.* **1980**, *102*, 5892-5902. (d) Johnson, C. D.; Roberts, I.; Taylor, P. G. *J. Chem. Soc., Perkin Trans.* **2** **1981**, 409-413.

(17) (a) le Noble, W. J.; Miller, A. R. *J. Org. Chem.* **1979**, *44*, 889-891. (b) Berg, U.; Gallo, R.; Metzger, J.; Chanon, M. *J. Am. Chem. Soc.* **1976**, *98*, 1260-1261. (c) Yamataka, H.; Ando, T. *Ibid.* **1979**, *101*, 266-267. (d) Abraham, M. H.; Nasehzadeh, A. *J. Chem. Soc., Chem. Commun.* **1981**, 905-906. (e) Harris, J. M.; Paley, M. S.; Prasthofer, T. W. *J. Am. Chem. Soc.* **1981**, 5915-5916. (f) Kevill, D. N. *J. Chem. Soc., Chem. Commun.* **1981**, 421-422. (g) Gallo, R. In "Progress in Physical Organic Chemistry"; Taft, R. W., Ed.; Wiley: New York, 1983. (h) Pross, A.; Shaik, S. S. *J. Am. Chem. Soc.* **1982**, *104*, 1129-1130 and references cited therein. (i) Kurz, J. L.; Seif El-Nasr, M. M. *Ibid.* **1982**, *104*, 5823-5824.

(18) Wolfe, S.; Mitchell, D. J.; Schlegel, H. B. *J. Am. Chem. Soc.* **1981**, *103*, 7692-7694, 7694-7696.

(19) Compare these results with the series of 2-methyl-3-alkylpyridines and 2-methyl-5-alkylpyridines studied by Brown and his students.^{6c-e}

Table X. Correlation Matrix for Experimental and GEOMO (MINDO/3)-Derived Parameters^{a, b}

	ΔE^\ddagger	ΔE_M	$\Delta H_{BF_3}^\circ$
$\ln k_2$	-0.877	-0.835	-0.901
ΔE^\ddagger		0.976	0.932
ΔE_M			0.914

^a See Table I for definitions of terms and units. Derived for 1-25 and 1C-25C. ^b All probabilities ≤ 0.00001 ; $n = 25$.

methylation activation energies relative to that of pyridine for 1-25 (ΔE^\ddagger , column three in Table I). The model transition states were treated in a fashion similar to that for the free bases and the cations. That is, with the single exception of the NC_M distance (which was kept at 1.88 Å), complete geometry optimization was performed with no symmetry restrictions.³ Using these results, we obtain (Figure 3 and eq 7) an excellent correlation between

$$\Delta H_{BF_3}^\circ = 1.00\Delta E^\ddagger + 0.53 \quad (7)$$

$$r = 0.932; p = 0.00001; n = 25; \text{std dev of residuals} = 0.938$$

Brown's observed heats of trifluoroboronation and our MINDO/3-generated methylation activation energies. These correlations support Brown's analogies⁶ regarding transition-state models (pyridine methylations) and steric effects in molecular addition compounds such as 9C, 26, and 27.

For comparative purposes, we show in Table X a correlation matrix for the experimentally obtained parameters and the MINDO/3-derived parameters. From the above, it follows that there is also a close relationship between ΔE^\ddagger and ΔE_M (eq 8) which can be interpreted as

$$\Delta E^\ddagger = 0.77\Delta E_M - 0.77 \quad (8)$$

$$r = 0.976; p < 0.00001; n = 25; \text{std dev of residuals} = 0.794$$

an approximation to the rate-equilibrium relationship (eq 9). The nonzero intercept in eq 8 is probably caused by

$$\Delta(\Delta G^\ddagger) = \alpha\Delta(\Delta G^\circ) \quad \text{where } 0 < \alpha < 1 \quad (9)$$

uncertainty in both the experimental data and theoretical energy calculations.

The requirement that α be between 0 and 1 indicates the fact that perturbations on equilibria are only partially reflected in the transition states. The coefficient of the ΔE_M term in eq 8 fulfills this requirement.^{17h}

The success of these linear energy relations (eq 6-8) indicates that there is a single predominant factor common to the three energy quantities ($\Delta H_{BF_3}^\circ$, ΔE_M , and ΔE^\ddagger). In this case, that common factor is almost certainly steric repulsion. Additional support for this conclusion will be discussed in the following section.

Because the MINDO/3-calculations were performed on both the pyridine free bases and the quaternary cations, the resultant correlations serve as additional validation for the use of the MINDO/3 algorithm for 1-25 and 1C-25C. These excellent correlations are particularly noteworthy given the structural diversity of 1-25 and the large range in reactivity of these pyridines; e.g., $\Delta\Delta E^\ddagger = 10.7$ kcal mol⁻¹. This observation is particularly interesting in light of recent ab initio calculations in which the relationship between activation parameters and thermodynamic pa-

rameters for S_N2 reactions is justified.¹⁸

Nonadditivity of Structure and Energetics

The additivity of substituent effects upon multiple substitution is of considerable interest. We will evaluate additivity in terms of the molecular geometries discussed above as well as in terms of the energetics of these pyridine alkylations.

To measure structural nonadditivity in the present data, we have defined the parameters δ_{\angle}^{FB} and δ_{\angle}^C for each multiply substituted free base and cation, respectively. Each parameter is the sum, over all six internal pyridine angles, of the absolute deviations of these angles between their optimized values and those predicted from the monosubstituted compounds on the basis of additivity. These nonadditive geometry parameters are listed in columns seven and eight of Table I for the free bases and the cations, respectively. We find essentially parallel behavior for δ_{\angle}^{FB} and δ_{\angle}^C . The only compounds that exhibit sizeable nonadditivities are the 2,3-disubstituted systems, and this can clearly be called a "buttressing" effect.

Nonadditivity of energetics is also apparent if one examines pairs of equivalently substituted 2-R,3-R' and 2-R,5-R' compounds. We can compare the parameters k_{rel} , ΔE^\ddagger , ΔE_M , and $\Delta H_{BF_3}^\circ$. In all cases, the 2-R,3-R' compound alkylates more slowly, has larger experimental and theoretical activation energies, and has a more positive heat of reaction than the corresponding 2-R,5-R' isomer.

We can also examine the nonadditive parts of these parameters for the multiply-substituted systems. These parameters are directly obtainable by using the monosubstituted molecule data as standards and are listed as S , $\Delta E^\ddagger(NA)$, $\Delta E_M(NA)$, and $\Delta H_{BF_3}^\circ(NA)$, respectively, in Table I. Since additivity of energies implies multiplicity of rate constants, the nonadditive kinetic factors, S , are defined as k_{rel} divided by the appropriate product of singly substituted k_{rel} values.²

The largest nonadditivity effects are displayed by the 2,3-disubstituted species and the 2,6-disubstituted systems. In contrast, 2,4- and 2,5-disubstituted pyridines which exhibit additivity in structure also show reasonable additivities for each of the energetic factors. This is consistent with the conclusion that nonadditivities are largely steric in nature.

In one examines pairs of equivalently substituted 2-R,3-R' and 2-R,5-R' compounds, interesting regularities emerge. In all cases, the nonadditive part of the molecular or chemical property is substantially greater for the 2-R,3-R'-substituted substrate than the corresponding 2-R,5-R' substrate. Furthermore, the difference increases as the bulkiness of the substituents increase.¹⁹ This is seen by examining in detail the information shown in Table I. These effects are seen for the kinetic nonadditivity factor, S , the nonadditive parts of the activation energies, $\Delta E^\ddagger(NA)$, the energies of methylation, $\Delta E_M(NA)$, the structural nonadditivity indicators, δ_{\angle}^{FB} and δ_{\angle}^C , and also in the nonadditive part of the experimental heats of trifluoroboronation, $\Delta H_{BF_3}^\circ(NA)$.

The introduction of specific bonding effects which change hybridization at several ring positions will almost certainly produce small perturbations at the other positions which should be additive in nature. Therefore, nonadditive steric parameters for 2-R,3-R'-substituted pyridines relative to 2-R,5-R' pyridines can be attributed to steric factors.

Nonadditivity is also observed, to a lesser extent, for the 2,6-dimethylpyridine and 2,4,6-trimethylpyridine systems. In general, the presence of two or more flanking groups which exhibit "buttressing" effects cause these observed

Table XI. Correlation Matrix of Nonadditive Parts^a of Experimental and GEOMO (MINDO/3)-Derived Parameters (Excluding 14, 15, 14C, and 15C)^b

	$\Delta E^\ddagger(\text{NA})$	$\Delta E_{\text{M}}(\text{NA})$	$\delta <^{\text{FB}}$	$\delta <^{\text{C}}$	$\Delta H_{\text{BF}_3}^\circ(\text{NA})$
$\ln S$	-0.894	-0.986	-0.804	-0.750	-0.970
$\Delta E^\ddagger(\text{NA})$		0.990	0.927	0.901	0.936
$\Delta E_{\text{M}}(\text{NA})$			0.928	0.903	0.930
$\delta <^{\text{FB}}$				0.989	0.855
$\delta <^{\text{C}}$					0.818

^a See Table I for definitions of terms and units. Derived for 1-13, 16-25, 1C-13C, and 16C-25C. ^b For analogous results derived for the entire sets 1-25 and 1C-25C, see Table XII.

nonadditivities. This result is quite reasonable, in that the net effect of adjacent bulky substituents will be other than one would predict on the basis of these groups behaving as if they were independent of each other. On the other hand, when the substituents are on opposite sides of the ring, their influence can be additive.

Table XI is a matrix of correlation coefficients between the six nonadditivity parameters, of which three derive from experimental data and three from theory. We derived Table XI excluding data for 2,6-dimethylpyridine and 2,4,6-trimethylpyridine for reasons discussed below. This is a rather subtle set of correlations in that we are examining the *nonadditive portions* of the parameters of interest. As can be seen from Table XI, there is substantial correlation between these nonadditive portions. Note, in particular, the significant correlations between the nonadditive portion of the MINDO/3 energy of methylation [$\Delta E_{\text{M}}(\text{NA})$] and the nonadditive portions of both the rate constants ($\ln S$) and the calculated activation energies [$\Delta E^\ddagger(\text{NA})$]. It is also interesting to note the correlation between $\ln S$ and the nonadditive portion of the heat of trifluoroboration [$\Delta H_{\text{BF}_3}^\circ(\text{NA})$].

An interesting intermediate case is 1,2,6-trimethylpyridinium cation (14C), for which reasonable structural additivity is observed simultaneously with kinetic and thermodynamic nonadditivity. Compare δ_2^{C} of 14C with those of 11C-13C. In this case, structural additivity is a consequence of the symmetrical molecular geometry. Minimum energy demands would require the N-CH₃ moiety to be distorted simultaneously away from both C₂-CH₃ and C₆-CH₃ (cf. Table VIII), a physical possibility assuming coplanarity of the methyl carbons and the ring. The expected structural changes tends to cancel one another, but the steric crowding leads to significant energetic nonadditivity. It is interesting to compare Table XI, which was derived for the polysubstituted pyridines excluding 2,6-dimethylpyridine (14) and 2,4,6-trimethylpyridine (15), with Table XII (see the paragraph at the end of the paper regarding supplementary material) which was derived for all the polysubstituted pyridines 11-25. Most of the correlations are considerably better without inclusion of 14, 15, 14C, and 15C. For example, the correlation coefficients of δ_2^{FB} with $\Delta E^\ddagger(\text{NA})$ and $\Delta E_{\text{M}}(\text{NA})$ are 0.927 and 0.928, respectively, when 14, 15, 14C, and 15C are excluded (Table XI) but are 0.792 and 0.844 when these 2,6-disubstituted pyridines are included.

Concluding Remarks

We have seen that substitution of alkyl groups for hydrogen atoms on pyridine and *N*-methylpyridinium cation causes significant ring geometry distortions. We have calculated these geometries using the MINDO/3 method with Rinaldi's geometry optimization procedure. More importantly, we have seen that multiple substitution on neighboring positions leads to appreciable nonadditivity in structural parameters. Corresponding nonadditivities have been observed in kinetic and thermodynamic pa-

rameters as well. The nonadditivities in the various parameters are well-correlated with one another. This leads us to the conclusion that there is one common cause for all the related effects, namely, steric repulsion.

The MINDO/3 method appears to be reasonably well-suited for the study of these systems, and, in particular, we conclude that it accounts satisfactorily for steric interactions and bonding interactions, at least in the systems considered here.

For the alkylation of substituted pyridines, the nonadditive effects lead to *less* reactivity, i.e., slower quaternization rates than would have been predicted on the basis of strict additivity.²⁶ This is quantitatively shown in Table I and is related to an *increased* amount of strain in the more crowded transition state and quaternary cation. In contrast, Röchardt and Beckhaus recently correlated the strength of the central carbon bond in substituted ethanes with the effect of substituents on bond angles, bond lengths, and conformations of these molecules.²⁰ In this latter situation, nonadditivity leads to *increased* reactivity, i.e., a faster rate of pyrolysis, since the transition states are less strained than the starting structures.

The observation that multiple substituents on an aromatic ring can cause structural parameter nonadditivity about the periphery of the ring (e.g., buttressing effects) is more well established²¹ than is the possibility that these substituents can cause significant change to the ring system itself. Typically the effects of substituents on aromatic ring geometry are ignored. We believe that evaluation of kinetic nonadditivities within a series of compounds may need to take into consideration variable and complex substituent-induced geometry changes to the "backbone" system itself.

Acknowledgment. We thank Dr. E. B. Sanders for his encouragement and support, K. McCourt and the Philip Morris Research Center Computer Group, in particular Drs. Victor Day and James Kao, for their assistance in this project, and M. Satterfield and P. Sinkiewicz for typing the manuscript. We also acknowledge the helpful suggestions and comments of the referees.

Registry No. 1, 110-86-1; 1C, 694-56-4; 2, 109-06-8; 2C, 18241-33-3; 3, 108-99-6; 3C, 18241-34-4; 4, 108-89-4; 4C, 18241-35-5; 5, 100-71-0; 5C, 60025-89-0; 6, 536-78-7; 6C, 52806-05-0; 7, 644-98-4; 7C, 59655-68-4; 8, 6304-18-3; 8C, 59564-32-8; 9, 5944-41-2; 9C, 85735-97-3; 10, 38031-78-6; 10C, 67508-12-7; 11, 583-61-9; 11C, 33718-16-0; 12, 108-47-4; 12C, 33718-17-1; 13, 589-93-5; 13C, 33718-18-2; 14, 108-48-5; 14C, 33718-19-3; 15, 108-75-8; 15C, 16344-86-8; 16, 14159-59-2; 16C, 85735-98-4; 17, 104-90-5; 17C, 60388-21-8; 18, 80263-42-9; 18C, 85735-99-5; 19, 20194-71-2; 19C, 85736-00-1; 20, 80263-43-0; 20C, 85736-01-2; 21, 85735-96-2; 21C,

(20) Röchardt, C.; Beckhaus, H.-D. *Angew. Chem., Int. Ed. Engl.* 1980, 19, 429-440.

(21) (a) Förster, H.; Vögtle, F. *Angew. Chem., Int. Ed. Engl.* 1977, 16, 429-441. (b) Paquette, L. A.; Gardlik, J. M. *J. Am. Chem. Soc.* 1980, 102, 5033-5035. (c) Paquette, L. A.; Hanzawa, Y.; Hefferon, G. J.; Blount, J. F. *J. Org. Chem.* 1982, 47, 265-272. (d) Leung, P.-L.; Curtin, D. Y. *J. Am. Chem. Soc.* 1975, 97, 6790-6799.

85736-02-3; 22, 56986-88-0; 22C, 85736-03-4; 23, 18113-81-0; 23C, 85736-04-5; 24, 72693-04-0; 24C, 85736-05-6; 25, 6343-58-4; 25C, 85736-06-7.

Supplementary Material Available: Table IV [GEOMO (MINDO/3)-derived ring geometries and total energies for sub-

stituted pyridines], Table V [GEOMO (MINDO/3)-derived ring geometries and total energies for substituted *N*-methylpyridinium cations] and Table XII [correlation matrix of nonadditive parts of experimental and GEOMO (MINDO/3)-derived parameters] (5 pages). Ordering information is given on any current masthead page.

Reduction of Azo-, Azoxy-, and Nitrobenzenes by Dihydrolipoamide-Iron(II)

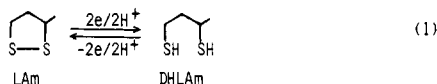
Masashi Kijima,* Yoko Nambu, Takeshi Endo, and Makoto Okawara

Research Laboratory of Resources Utilization, Tokyo Institute of Technology, Nagatsuta, Midori-ku, Yokohama 227, Japan

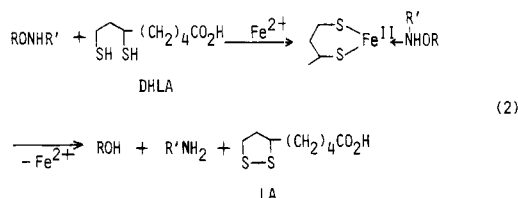
Received October 13, 1982

Dihydrolipoamide (DHLAm) was found to be an effective reagent for the reduction of nitrobenzene derivatives in the presence of a catalytic amount of ferrous ion. Azo- and azoxybenzenes were reduced to hydrazobenzene without the formation of aniline, and nitrobenzene, nitrosobenzene, and phenylhydroxylamine were also reduced to aniline in good yields under mild conditions. The reduction was presumed to proceed through the complex formation between DHLAm, ferrous ion, and substrates.

Lipoamide (LAm) works as a coenzyme related to acyl-transfer and redox reactions in living systems based on a redox function of LAm \rightleftharpoons dihydrolipoamide (DHLAm) (eq 1). We have studied¹ applications of LAm de-



rivatives for acyl-transfer reactions. We have also reported² that hydroxylamines are cleaved reductively to give corresponding amines and alcohols by dihydrolipoic acid (DHLA) through the coordination of substrates to a 1:1 complex of DHLA-Fe(II), as shown in eq 2. The reduc-



tion system seems to have mechanistic interest due to the reactivity of the dithiol-iron complex related to non-heme iron proteins such as rubredoxins and ferredoxins in living systems.

In this paper, we describe the reduction of azo-, azoxy-, and nitrobenzenes by the DHLA or DHLAm (DHLAs)-Fe(II) system.

Results and Discussion

The reactivity of the DHLAs-Fe(II) system for the reduction of various functional groups was preliminarily investigated by spectrophotometric methods. As described² in the reductive cleavage of hydroxylamine derivatives by DHLAs-Fe(II), the progress of the reduction could be monitored by the appearance of UV absorption (λ_{max} 333 nm) due to the 1,2-dithiolane ring of LA or LAm,

Table I. Reduction of Azobenzene by DHLAs-Fe(II)^a

[reducing agent], M		% yield of hydrazobenzene ^b
DHLAs	Fe ²⁺	
1 × 10 ⁻¹ (DHLAm)	5 × 10 ⁻⁴	90 (80) ^c
1 × 10 ⁻¹ (DHLA)	5 × 10 ⁻⁴	9
1 × 10 ⁻¹ (DHLAm)	0	0
0	1 × 10 ⁻¹	0

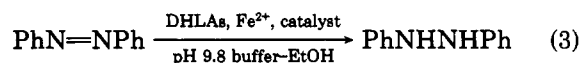
^a Conditions: [azobenzene] = 5 × 10⁻² M, 0.2 M carbonate buffer (pH 9.8)-EtOH (1:3), 30 °C, 24 h.

^b Determined by ¹H NMR method. ^c Isolated yield.

which were produced during the reduction. The reductions of some compounds by DHLAs were now attempted in the presence of a catalytic amount of ferrous ion, and the change of UV absorption was followed. No UV absorption change at 333 nm was observed in the reduction of activated olefin (cinnamyl alcohol), ketone (cyclohexanone), and aldehyde (benzaldehyde). In the case of the reduction of azo-, azoxy-, and nitrobenzenes by DHLAm-Fe(II), the formation of LAm was observed by UV absorption change, which suggested the progress of the reduction. We investigated in detail the reduction of azo-, azoxy-, nitrobenzene, and related compounds by DHLAm-Fe(II).

Reduction of Azobenzene by DHLAm-Fe(II). The reduction of azobenzene was carried out by DHLAm in the presence of a catalytic amount of ferrous ion in 0.2 M carbonate buffer (pH 9.8)-ethanol (1:3) under an argon atmosphere at 30 °C for 24 h. The results are summarized in Table I together with those for the DHLA-Fe(II) system.

Azobenzene was found to be reduced to hydrazobenzene almost quantitatively by DHLAm-Fe(II) under mild conditions without the formation of aniline (eq 3). On



the other hand, no reduction occurred when an equimolar amount of either DHLAm or ferrous ion was used. These results suggest that in the reduction of azobenzene the DHLAm-Fe(II) complex is an active species in analogy with the reduction of hydroxylamine derivatives.² Azo-

(1) Nambu, Y.; Endo, T.; Okawara, M. *J. Polym. Sci., Polym. Chem. Ed.* 1980, 18, 2793; 1981, 19, 1937.

(2) Nambu, Y.; Kijima, M.; Endo, T.; Okawara, M. *J. Org. Chem.* 1982, 47, 3066.